Advanced Composites and Hybrid Materials (2021) 4:647–661
https://doi.org/10.1007/s42114-020-00185-x

ORIGINAL RESEARCH

Determination of thermal conductivity of bamboo plyboard as thermal insulator for passive roof cooling

Estrella C. Macabutas[1,2] · **Alejandro F. Tongco**[1]

Received: 23 May 2020 / Revised: 24 September 2020 / Accepted: 13 October 2020 / Published online: 24 October 2020

Abstract
Two samples of each of different local bamboo species in the treated and untreated conditions were prepared. They are of the species *Dendrocalamus merrillianus* (Bayog), *Schizostachyum lumampao* (Buho), *Bumbusae* (Kawayan), and *Bambusa vulgaris* (Patong). These samples were used to determine their fire resistance property. The fire resistance criterion was the time required for the samples to burn completely. Sample preparation entails pulverization of the bamboo to a fine-grain sawdust structure, then formed into a board structure. Each bamboo species type was made into the bamboo board (herein referred to as the *plyboard*) with one sample treated with mango polyphenol extract while the other was left untreated. The result of the fire-resistant tests shows that *Bambusa vulgaris* (Patong) treated with 10% mango polyphenol extract has the highest fire resistance, implying good insulating property. The scope of this study is limited only for the fire resistance determination and the consequent determination of the thermal conductivity of the selected material in its plyboard form. The thermal conductivity ranges from 0.000 to 0.098 W/m K and the average mean is 0.032 W/m K. It was also concluded that the thermal conductivity in 3 consecutive days and every 4 h was a high correlation. It rejects the null hypothesis; so, therefore, there is a significant difference between thermal conductivity and temperature of bamboo ply. The average mean has a low thermal conductivity, implying that sawdust bamboo ply made of *Bambusa vulgaris* (Patong) treated with mango polyphenol extract has good insulating value.

Keywords Bamboo · Fire resistance · Passive roof cooling · Thermal conductivity

1 Introduction

Sawdust bamboo ply is a green material that could be used as an insulator for the roof module to provide thermal comfort cooling of the house with no energy to operate. Studies show that using and utilizing green materials reduce carbon dioxide concentration, which results in global warming. The usage of safe, clean, and desirable materials is a favorable strategy for environmental remediation [1, 2]. The efficiency of green technology has been contributing to the advantageous effect on human life [1]. Green synthesis is an eco-friendly material which is naturally available. Many studies utilized the green chemistry and greener approach for the fabrication of new non-hazardous compounds to eliminate the harmful ingredients to the human health and for the safety of the environment [3–5]. Nowadays, the application of green chemistry is more advantageous because of the low cost, being a naturally available material, and non-toxicity reagents [6]. Studies show that the use of green materials as roof insulators for the roof module is better than of standard air conditioning, because of no fuel required and not producing CO_2 concentration but more comfort cooling of the house especially during summer months. To reduce the carbon dioxide emission, green and renewable raw materials could be utilized all over the world especially in the Philippine country. It can help also forecast the possible scenarios in the future that would help prepare, mitigate, and adapt to this emerging environment. A sawdust bamboo ply is proposed as a thermal insulator and a composite part of the roof module for passive roof cooling.

Passive roof cooling methods using green materials as a thermal insulator use simple mechanism and no electricity required. During night time, passive cooling affects the roof

✉ Estrella C. Macabutas
macabutasestrella@gmail.com

Alejandro F. Tongco
aftongco@usc.edu.ph

1 School of Engineering, University of San Carlos, Talamban Campus, 6000 Cebu City, Philippines

2 Western Philippines University, 5302 Aborlan, Palawan, Philippines

through radiation to the night sky using the roof module as a heat sink based on the principle of heat loss by longwave radiation [7, 8]. Roof insulation using green materials is a big help to reduce the heat inside the house not only for night time but also for day time. By improving the thermal performance of roof, the thermal conductivity of sawdust bamboo ply was determined.

The thermal conductivity, k (W/m^2 K), of a material is the rate of heat transfer through a unit thickness of the material per unit temperature difference [9], given by Eqs. 1 and 2, where Q_{cond} is the heat conduction in watts, A is the surface area in m^2, x in m, and ΔT is a temperature gradient in Kelvin. At steady-state conditions, heat is conducted in the direction of decreasing temperature and hence, the temperature gradient $(T_2 - T_1)$ is negative when temperature decreases in the positive direction [9] (see Eq. 1 for heat conduction)

$$Q_{\text{cond}} = -kA\frac{\Delta \text{T}}{\text{x}} \tag{1}$$

Equation 1 describes heat conduction which is called Fourier's law. A layer of material of known thickness and area can be heated from one side by an electric resistance heater of known output. If the outer surfaces of the heater are well insulated, all the heat generated by the resistance heater is transferred through the material whose conductivity is to be determined. Thus, thermal conductivity is a product of the heat conduction and thickness of the material and the quotient of the cross-sectional area and temperature gradient through the body of mass described by Eq. 2 [9]. Together with other known quantities given, the thermal conductivity is shown in Fig. 1.

$$\text{k} = \frac{\text{Q}_{cond}x}{A\Delta T} \tag{2}$$

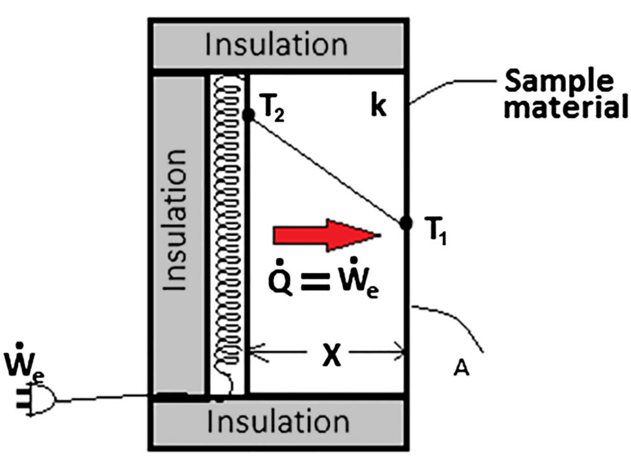

Fig. 1 Illustration of thermal conductivity

There are three ways in which heat is transferred from one body to another. These are conduction, convection, and radiation. In Fig. 1, conduction occurs within a solid or between the bodies in intimate contact with each other. Natural or free convection is the heat transfer due to fluid motion caused by buoyant forces, while forced convection occurs when a fan or pump impels the fluid to flow. Natural convection is classified further depending on whether the developed fluid flow is laminar or turbulent. The fluid flow is assumed to be laminar [9, 10]. Despite the complex behavior of convection, it is described by the simple relation known as Newton's law of cooling, as shown in Eq. 3:

$$\text{Q}_{conv} = hA(T_{sur} - T_{amb}) \tag{3}$$

where T_{sur} is the surface temperature in °C and T_{amb} is the ambient temperature in °C, A is the surface area in m^2, and h is the convective heat transfer coefficient in W/m^2 °C [10]. In the absence of fluid forces caused by wind or a fan, the convective heat transfer that takes place is called natural convection. Natural convection is due to the buoyant force, which is the force exerted on a body or a volume of the fluid, by a surrounding fluid. The buoyancy force equals the weight of the fluid displaced by the body or fluid volume [9, 10].

On the other hand, radiation is the energy transferred between bodies not in contact with each other and may or may not have a medium in between them for radiant energy transfer to take place [9, 10]. The radiant energy exchange between the G.I. roof surface and the night sky may be determined by Eq. 4 [8]:

$$Q_{skyrad}/A = \varepsilon_r \sigma \left[\left(T_{roof}\right)^4 - \left(T_{sky}\right)^4 \right] \tag{4}$$

Equation 4 is the heat flux or the heat rate per unit area expressed in Joules per second per square meter of surface (or watts per square meter), where ε_r is the long-wave emissivity of the radiating surface in dimensionless quantity, σ is the Stefan-Boltzmann constant (5.67×10^{-8}W/m^2 K^4), T_{roof} is the absolute temperature of the radiating surface in Kelvin degrees, and T_{sky} is the absolute effective sky temperature in Kelvin degrees. It is the heat loss of the roof top to the sky by radiation [8]. This will ultimately result in the increased cooling of the naturally recirculated air through the airgap, and more ventilation air flows into the interior of the house. Sky temperature T_{sky} is presented in Eq. 5 [7] for estimating the sky emissivity and temperature, where T_{amb} is the ambient temperature in °C and ε_{sky} is the emissivity of the sky as described in Eq. 6 [7], where t_{dp} is the dew point temperature in °C.

As can be deduced from Eq. 6 [7], the higher the dew point temperature of the air, the higher is the emissivity, and the lower the temperature of the air, the lower is the effective sky temperature. It follows that for cooling to take place the sky must have a lower temperature than that of the roof. The radiation potential $\left(T_{sky}^4 - T_{roof}^4\right)$ will produce no cooling if the value is zero, and cooling when the value is negative; otherwise, the roof will be heated. The greater the negative difference, the greater will be the cooling effected.

$$T_{sky} = T_{amb}\left(\varepsilon_{sky}{}^{0.25}\right) \tag{5}$$

$$\varepsilon_{sky} = 0.711 + 0.56\left(t_{dp}/100\right) + 0.73\left(t_{dp}/100\right)^2 \tag{6}$$

$$t_{dp} = C_{14} + C_{15}\alpha + C_{16}\alpha^2 + C_{17}\alpha^3 + C_{18}(P_w)^{0.1948} \tag{7}$$

$$\alpha = ln\left(P_w\right) \tag{8}$$

$$P_w = \frac{P_{atm}W}{0.621\,945 + W} \tag{9}$$

$$W = \frac{\left(2501 + 2.326t^*\right)W_s{}^* - 1.006\left(t_{amb} - t^*\right)}{2501 + 1.86t_{amb} - 4.186t^*} \tag{10}$$

$$W_s{}^* = 0.621\,945\,\frac{P_w{}^*}{P_{atm} - P_w{}^*} \tag{11}$$

Also, Eq. 7 is for determining the dew point temperature of the air [11], where $C_{14} = 6.54$, $C_{15} = 14.526$, $C_{16} = 0.7389$, $C_{17} = 0.09486$, and $C_{18} = 0.4569$, and α is given in Eq. 8, where P_w is the partial pressure of water vapor in unsaturated air in kPa units [11]. Equation 10 may be used for obtaining the humidity ratio of the unsaturated air. The partial pressure of water vapor P_w is described in Eq. 9, where P_{atm} is the total pressure of moist air in kPa (atmospheric pressure, 101.325 kPa at sea level) and W is the humidity ratio of unsaturated air in $kg_{w.v.}/kg_{d.a}$ [11]; where t^* is the thermodynamic low temperature of moist air taken from PAGASA in °C and $W_s{}^*$ is the humidity ratio of moist air at saturation based on saturation temperature in $kg_{w.v.}/kg_{d.a.}$ in Eq. 11 [11], where $P_w{}^*$ is the saturation pressure based on vapor pressure of the air, in kPa unit.

There are several reports on green synthesis on the various kinds of biofuel nanoscale compounds for utilizing clean energy in alleviating pollution conditions by production of nanostructured compounds [1–6]. Carbon dioxide emission on earth causes greenhouse effect which contributes to global warming. The Philippines is one of the highly urbanized country in the world, with establishments such as malls, hotels, restaurants, and even residential houses using electricity-driven air-conditioning system to provide comfort cooling to occupants. Today, the challenge is the sustainability for thermal comfort cooling without the use of air-conditioning system. Building owners may not be aware that there are other means of providing comfort, and the utilization of alternative but efficient green materials (bamboo plyboard) as thermal insulation.

Bamboo has been known as a material for environmental building for its abundance and low cost [12]. It is an energy-saving material when used as an air-conditioning insulation [13]. In Japan and China, bamboo is one of the oldest and an adaptable material that was used for more than 2000 years. Today, in Latin-America and Asia, bamboo is increasingly used for the construction of light structures [14].

The objective of this study is the indirect determination of the (a) fire resistance quality and (b) thermal conductivity of bamboo plyboard by retrofitting it to a system (like the roof module) where its thermal performance as a conductor of heat can be simulated. The result of the study shows the highest assessed lapse time among the different bamboo species after it burned. There are four species of bamboo to test the fire resistance, with treatment of mango polyphenol extract and without treatment; those are the *Dendrocalamus merrillianus* (Bayog), *Schizostachyum lumampao* (Buho), *Bumbusae* (Kawayan), and *Bambusa vulgaris* (Patong). The fire resistance criterion used was the time for a sample to completely burn, assuming all ambient conditions to be the same for each test. The sample with the longest time to burn implies highest fire resistance and was eventually selected and then fabricated into a plyboard (finished product). After the fire resistance test and plyboard fabrication, the next step was to determine the thermal conductivity of the plyboard. A roof module consists of corrugated G.I. sheet at the top, an airgap below acting as flow channel for air, and insulation made of green materials (bamboo plyboard) located below the airgap. In other words, the airgap separates the G.I. roof sheet from the insulation layer to form a parallel plate channel. Mathematical equations for a one-dimensional and steady-state heat transfer across this roof system were derived. This derived equations or formulas are used to predict the temperatures at the different points in the roof and surface temperature of sawdust bamboo ply as well as the heat fluxes across the roof. The input to this module is the temperature sent through the subscriber identification module (SIM) using the Arduino based on the weather ambient temperature. This study provides illustrations and discussion of materials and methods used in this experimental study.

2 Materials and methods

The paradigm in Fig. 2 shows the methods of the study. *Dendrocalamus merrillianus* (Bayog), *Schizostachyum*

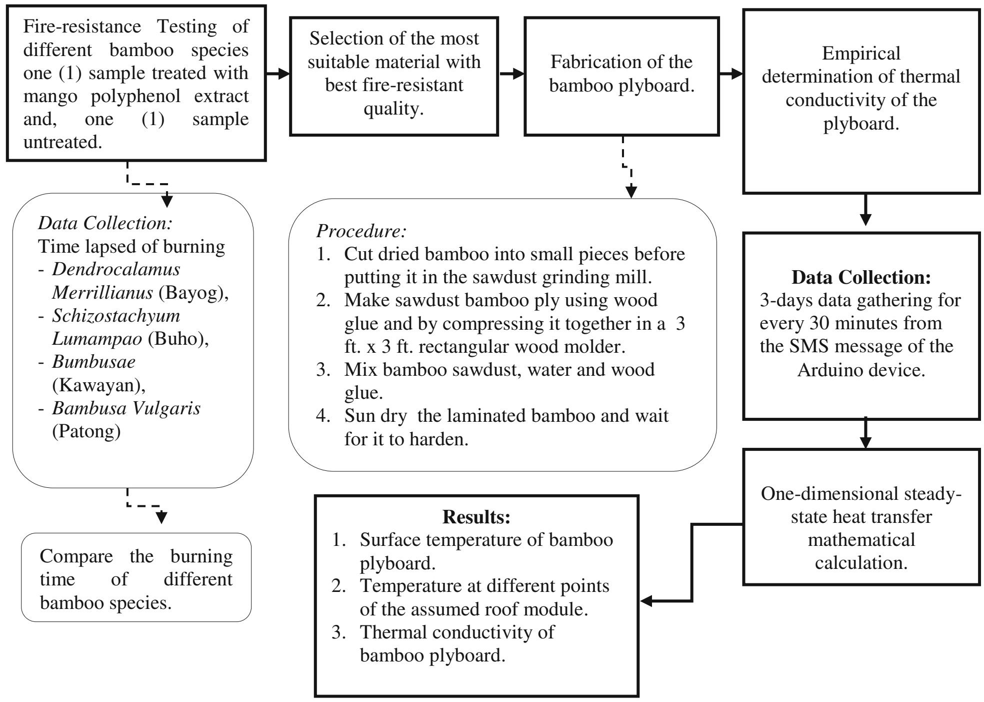

Fig. 2 Paradigm of methodology

lumampao (Buho), *Bumbusae* (Kawayan), and *Bambusa vulgaris* (Patong) are endemic bamboo species of the Philippines. The harvested bamboo went through three processes. The first treatment was controlled air-drying; second, soaking the bamboo in salt water for 7 days; and third, soaking with saltwater plus 10% solution of mango polyphenol extract within 7 days. The untreated bamboo sample was in its natural state. On the last day of curing, the samples were set up into the dry cans. The bamboo was weighed and set on fire and burning time per sample eventually recorded. The higher fire resistance was then ground to fine-grained sawdust size in a grinding mill. After it was made into sawdust, the coarse chunks of bamboo were screened out, using a sieve.

The fabrication materials and tools used are (1) wood glue, (2) mixing bowl, (3) trowel, (4) wooden frame, (5) plastic-covered illustration boards for the molding process as shown in Fig. 3, (6) and additional bench tools and measuring instruments that can be used in the process. On the illustration board, we start by using small amounts of the mixture using the wooden frame, and then flatten the mixture with a trowel. After the mixture has been molded into a sheet, it was left to settle and dry completely for 4 days. The bamboo plyboard was retrofitted into the roof module as a ceiling material.

The Arduino device was then put into action. It sends the surface temperature measurements of every key points along the roof module every 30 min (inner and outer G.I. roof,

Fig. 3 Procedures in making bamboo plyboard

airgap, and inner and outer ceiling board made of bamboo plyboard). Surfaces and interface temperatures are evaluated based on the rearranged version of Eqs. 17–21. The thermal resistance can still be used to determine the rate of steady heat transfer through such composite roofing. The roofing consists of three layers (such as roof, airgap, and ceiling board made of green materials). We could also obtain this result by following the approach already used previously to obtain the outer roof surface temperature t_5 by the premise that the rate of heat transfer Q_{total} through a multi-layer medium is constant, and thus, it must be the same through each layer. The temperature at the airgap t_3 was from Arduino device sent via SMS. A roof module consisting of corrugated G.I. sheet, airgap, and insulation made of green materials (sawdust bamboo ply) is shown in Fig. 4.

Figure 4 describes the corrugated roof (G.I. sheet, gauge no. 24) having a low pitch (or slope) of 2/12 (approximately 9.46 degrees). The peak of the roof joins a vertical wall with an airgap underneath to represent a tilted channel formed between two parallel plates. Warm air circulates through the interior of the house, flows through the 0.84 m (0.75 inches) deep airgap, giving its heat to the roofing, and flows downward at exceptionally low rates. Because of the thickness of the airgap, the natural convection is somewhat suppressed, and the heat transfer is by conduction alone. The warm air at airgap losses some of its heat to the G.I. sheet. The sky and the ambient air serve as the heat sink for the system. The massive construction of interior tiled floors and concrete walls stores sensible cooling to reduce night-time space conditioning needs. The bamboo plyboard isolates the air in the cooling chamber (or airgap) from the warm room air.

Figure 5 represents the system of concern, in which the mean surface temperature of the roof is greater than the outside ambient temperature. Heat flows up from air in the airgap to the G.I. roofing in a steady-state, steady flow (SSSF), unidirectional flow of heat, and without condensation occurring. The term steady-state implies no property change with time at any point in the system. The outdoor condition t_{amb} was based on the average of 24-h operation.

The modes of heat transfer shown in Fig. 5 are radiation from room wall and flooring to sawdust bamboo ply, longwave radiation from G.I. roof to the sky, convection from room air to bamboo plyboard, convection from G.I. roof outer surface to outside air, and conduction from sawdust bamboo ply insulation to airgap and conduction from sawdust bamboo ply to inner roof. Figure 5 shows one-dimensional heat transfer by conduction, convection, and radiation through composite roof assembly exposed to temperatures t_{amb} and t_r which can be express as [10]:

$$Q_{total} = \frac{\Delta t_{ave}}{R_{total}} = \frac{(t_r - t_{amb})_{ave}}{R_{total}} \tag{12}$$

The total heat toward the outside (indicating heat loss) from hot to cold medium is given by Eq. 12 [9], where Δt_{ave} is the total temperature between the two mediums in °C, R_{total} is the total thermal resistance between the two mediums in °C/W, t_r is the room temperature in °C, and t_{amb} is the ambient temperature in °C. For the composite system, the overall resistance is [10]:

$$R_{total} = R_{room} + R_{bp} + R_{ag} + R_{roof} + R_{sky} \tag{13}$$

or

$$R_{total} = \frac{1}{\left(\frac{1}{R_{rad}} + \frac{1}{R_{conv}}\right)_{room}} + R_{bp} + R_{ag} + R_{roof} + \frac{1}{\left(\frac{1}{R_{rad}} + \frac{1}{R_{conv}}\right)_{sky}} \tag{14}$$

Substituting the values, we have

$$R_{total} = \left[\frac{h_i + h_{rad}}{h_i h_{rad} A}\right]_{room} + \frac{x_{bp}}{k_{bp} A} + \frac{x_{ag}}{k_{air} A} + \frac{x_{roof}}{k_{roof} A} + \left[\frac{h_o + h_{rad}}{h_o h_{rad} A}\right]_{sky} \tag{15}$$

The heat transfer surface area is constant for the roof assembly. The thermal resistances are all in series, and the equivalent total thermal resistance is determined by adding the individual resistances. The outside air temperature t_{amb} is a temperature from the Philippine Atmospheric, Geophysical, and Astronomical Services Administration (PAGASA). The t_{room} is the assumed value of mean temperature at room (32 °C). Since the composite heat rate is unidirectional, steady-flow, and [10]

$$t_{room} - t_{amb} = (t_{room} - t_1) + (t_1 - t_2) + (t_2 - t_4) + (t_4 - t_5) + (t_5 - t_{amb}) \tag{16}$$

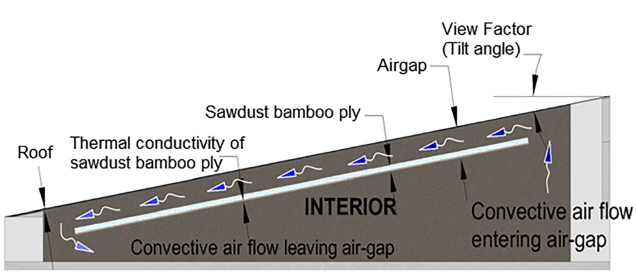

Fig. 4 Schematic concept of a roof module with bamboo plyboard as an insulator

Fig. 5 Thermal model of the roof module

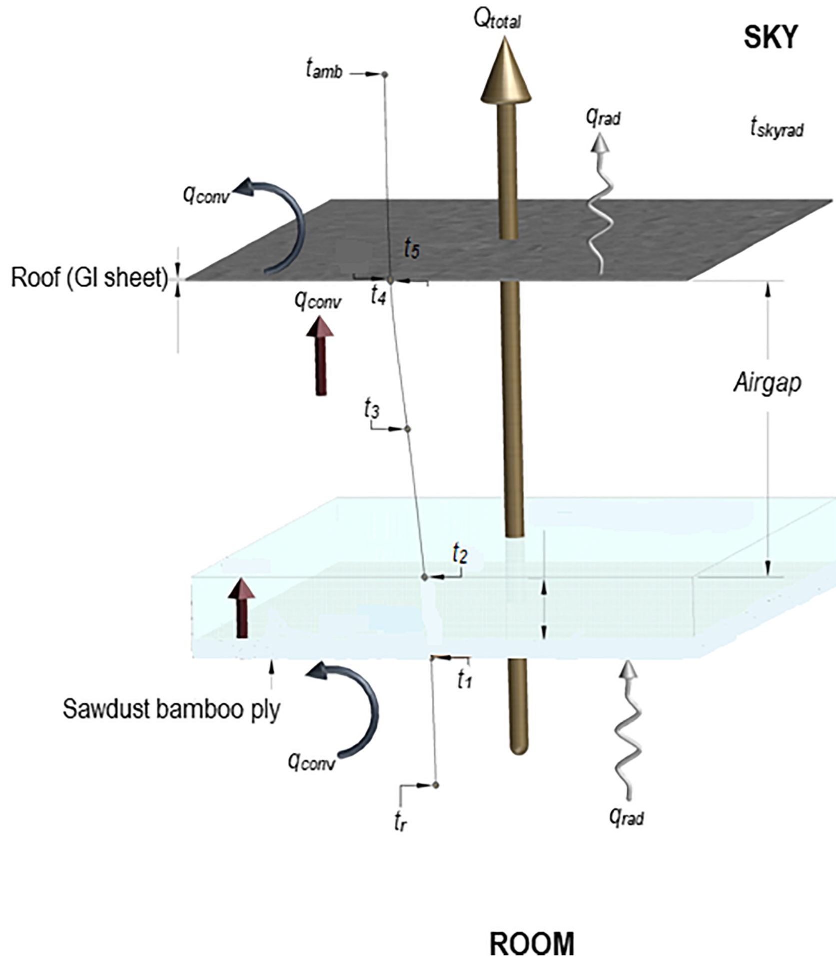

Then, the total heat flow is described by Eqs. 17–21.

$$Q_{total} = \frac{t_{room} - t_1}{R_{room}} \quad (17)$$

$$Q_{total} = \frac{t_1 - t_2}{R_{bp}} \quad (18)$$

$$Q_{total} = \frac{t_2 - t_4}{R_{ag}} \quad (19)$$

$$Q_{total} = \frac{t_4 - t_5}{R_{roof}} \quad (20)$$

$$Q_{total} = \frac{t_5 - t_\infty}{R_{sky}} \quad (21)$$

Table 1 Fire resistance for sample no. 1

Treated/untreated	Bamboo species	Weight of bamboo (g)	Weight of ash (g)	Time lapse (min)
Treated with polyphenol	Bayog	1900	1100	14 min 32 s
Untreated	Bayog	1900	1100	12 min 12 s
Treated with polyphenol	Patong	1880	1010	15 min 32 s
Untreated	Patong	1880	1010	11 min 39 s
Treated with polyphenol	Buho	1990	1210	11 min 11 s
Untreated	Buho	1990	1205	8 min 55 s
Treated with polyphenol	Kawayan	1185	870	08 min 6 s
Untreated	Kawayan	1185	870	08 min 23 s

Table 2 Fire resistance for sample no. 2

Treated/untreated	Bamboo species	Weight of bamboo (g)	Weight of ash (g)	Time lapse (min)
Treated with polyphenol	Bayog	1500	1000	11 min 32 s
Untreated	Bayog	1500	1000	09 min 17 s
Treated with polyphenol	Patong	1600	1010	12 min 12 s
Untreated	Patong	1600	1020	10 min 02 s
Treated with polyphenol	Buho	1500	1010	10 min 11 s
Untreated	Buho	1500	1005	08 min 55 s
Treated with polyphenol	Kawayan	1500	1010	07 min 16 s
Untreated	Kawayan	1500	1005	07 min 27 s

Resistances in parallel:

$$R_{room} = \frac{1}{\left(\frac{1}{R_{rad}} + \frac{1}{R_{conv}}\right)_{room}} \tag{22}$$

where $R = 1/hA$; then,

$$R_{room} = \frac{1}{\frac{1}{\frac{1}{h_{rad}A} + \frac{1}{h_iA}}} \tag{23}$$

Rearranged the equation [23]:

$$R_{room} = \frac{1}{\frac{1}{\frac{h_iA + h_{rad}A}{h_ih_{rad}A^2}}} \tag{24}$$

therefore,

$$R_{room} = \left(\frac{h_i + h_{rad}}{h_ih_{rad}A}\right)_{room} \tag{25}$$

and

$$R_{sky} = \left(\frac{h_o + h_{rad}}{h_oh_{rad}A}\right)_{sky} \tag{26}$$

where R_{room} is the total resistance to flow of heat from occupants to plywood surface in °C/W, R_{sbp} is the resistance to flow of heat by sawdust bamboo ply with thickness x_{sbp} in °C/W, $R_{ag}$is the resistance to flow of heat by the air at airgap with thickness x_{ag} in °C/W, R_{roof} is the resistance to flow of heat by the G.I. roofing material with thickness x_{roof} in °C/W, and R_{sky} is the total resistance to flow of heat from roof to sky in °C/W. The commonly used value of h_o for peak load calculation is 22.7 W/m^2 °C (summer) which corresponds to design wind conditions of 12 km/h for summer. And, the commonly used value of h_i for peak load calculation is 8.29 W/m^2 °C (winter and summer), which corresponds to design wind conditions of 12 km/h for summer [10].

The data of the null hypothesis of the correlation coefficient uses QI Macros Statistic Wizard and Minitab software for the accurate result of correlation.

Table 3 Fire resistance for sample no. 3

Treated/untreated	Bamboo species	Weight of bamboo (g)	Weight of ash (g)	Time lapse (minutes)
Treated with polyphenol	Bayog	1500	860	11 min 32 s
Untreated	Bayog	1500	840	09 min 17 s
Treated with polyphenol	Patong	1600	980	12 min 12 s
Untreated	Patong	1600	970	10 min 02 s
Treated with polyphenol	Buho	1500	770	10 min 11 s
Untreated	Buho	1500	750	08 min 55 s
Treated with polyphenol	Kawayan	1500	710	07 min 16 s
Untreated	Kawayan	1500	700	07 min 27 s

Table 4 Thermal conductivity of bamboo plyboard at environmental temperature (t_1) of 32 °C (305.15 K)

Date	Time, *t* min (every 30 min)	Temp.@ pt. 1 (t_1, °C)	Temp. @ pt. 2 (t_2, °C)	Temp. @ pt. 3 reading in the Arduino device (t_3, °C)	Temp. @ pt. 4 (t_4, °C)	Temp. @ pt. 5 (t_5, °C)	Room temp., t_r, °C	Thermal conductivity, k (W/m K)
9-Mar-19								
	8:56	32	28.02	26	30.04	30.04	32.05	0.012
	9:29	32	28.02	26	30.04	30.04	32.05	0.012
	9:57	32	28.52	27	30.04	30.04	32.05	0.011
	10:27	32	29.02	28	30.04	30.04	32.05	0.009
	11:28	32	29.52	29	30.04	30.04	32.05	0.008
	11:58	32	29.52	29	30.04	30.04	32.05	0.008
	12:28	32	30.51	30	31.02	31.02	32.02	0.002
	12:59	32	31.01	31	31.02	31.02	32.02	0.002
	13:29	32	31.51	32	31.02	31.02	32.02	0.001
	13:59	32	32.51	34	31.02	31.02	32.02	-0.001
	14:30	32	32.51	34	31.02	31.02	32.02	-0.001
	15:00	32	32.51	34	31.02	31.02	32.02	-0.001
	15:31	32	31.51	34	31.02	31.02	32.02	0.001
	16:02	32	31.51	32	31.02	31.02	32.02	0.001
	16:31	32	30.01	32	31.02	31.02	32.02	0.003
	17:02	32	30.01	29	31.02	31.02	32.02	0.003
	17:32	32	30.01	29	31.02	31.02	32.02	0.003
	18:12	32	28.05	29	27.11	27.10	32.12	0.031
	18:33	32	28.05	29	27.11	27.10	32.12	0.031
	19:03	32	28.05	29	27.11	27.10	32.12	0.031
	19:33	32	27.55	28	27.11	27.10	32.12	0.034
	20:04	32	27.05	27	27.11	27.10	32.12	0.038
	20:34	32	27.05	27	27.11	27.10	32.12	0.038
	21:04	32	27.05	27	27.11	27.10	32.12	0.038
	21:35	32	27.05	27	27.11	27.10	32.12	0.038
	22:05	32	27.05	27	27.11	27.10	32.12	0.038
	22:35	32	27.05	27	27.11	27.10	32.12	0.038
	23:06	32	26.55	26	27.11	27.10	32.12	0.042
	23:36	32	26.55	26	27.11	27.10	32.12	0.042
10-Mar-19								
	0:06	32	25.09	26	24.18	24.17	32.19	0.086
	0:37	32	25.09	26	24.18	24.17	32.19	0.092
	1:07	32	24.59	25	24.18	24.17	32.19	0.092
	1:38	32	24.59	25	24.18	24.17	32.19	0.092
	2:08	32	24.59	25	24.18	24.17	32.19	0.092
	2:38	32	24.59	25	24.18	24.17	32.19	0.092
	3:09	32	24.09	24	24.18	24.17	32.19	0.098
	3:39	32	24.09	24	24.18	24.17	32.19	0.098
	4:09	32	24.09	24	24.18	24.17	32.19	0.098
	4:40	32	24.09	24	24.18	24.17	32.19	0.098
	5:10	32	23.59	23	24.18	24.17	32.19	0.104
	5:40	32	23.59	23	24.18	24.17	32.19	0.104
	6:11	32	26.52	23	30.04	30.04	32.05	0.017
	6:41	32	26.52	23	30.04	30.04	32.05	0.017
	7:11	32	26.52	23	30.04	30.04	32.05	0.017

Table 4 (continued)

Date	Time, *t* min (every 30 min)	Temp.@ pt. 1 (t_1, °C)	Temp. @ pt. 2 (t_2, °C)	Temp. @ pt. 3 reading in the Arduino device (t_3, °C)	Temp. @ pt. 4 (t_4, °C)	Temp. @ pt. 5 (t_5, °C)	Room temp., t_r, °C	Thermal conductivity, k (W/m K)
	7:42	32	26.52	23	30.04	30.04	32.05	0.017
	8:12	32	26.52	23	30.04	30.04	32.05	0.017
	8:42	32	27.02	24	30.04	30.04	32.05	0.015
	9:13	32	27.52	25	30.04	30.04	32.05	0.014
	9:43	32	28.02	26	30.04	30.04	32.05	0.012
	10:13	32	28.52	27	30.04	30.04	32.05	0.011
	10:44	32	29.02	28	30.04	30.04	32.05	0.009
	11:15	32	29.52	29	30.04	30.04	32.05	0.008
	11:45	32	29.52	29	30.04	30.04	32.05	0.008
	12:15	32	30.02	30	30.04	30.04	32.05	0.006
	12:45	32	30.02	30	30.04	30.04	32.05	0.006
	13:16	32	31.02	32	30.04	30.04	32.05	0.003
	13:46	32	32.02	34	30.04	30.04	32.05	0.000
	14:16	32	32.52	35	30.04	30.04	32.05	-0.002
	14:47	32	32.52	35	30.04	30.04	32.05	-0.002
	15:17	32	32.52	35	30.04	30.04	32.05	-0.002
	15:47	32	31.52	35	30.04	30.04	32.05	0.001
	16:18	32	31.02	32	30.04	30.04	32.05	0.003
	16:48	32	31.02	32	30.04	30.04	32.05	0.003
	17:18	32	30.52	31	30.04	30.04	32.05	0.005
	17:49	32	29.52	29	30.04	30.04	32.05	0.008
	18:19	32	28.05	29	27.11	27.10	32.12	0.031
	18:51	32	28.05	29	27.11	27.10	32.12	0.031
	19:20	32	27.55	28	27.11	27.10	32.12	0.034
	19:50	32	27.55	28	27.11	27.10	32.12	0.034
	20:51	32	27.05	27	27.11	27.10	32.12	0.038
	21:21	32	27.05	27	27.11	27.10	32.12	0.038
	21:52	32	26.55	26	27.11	27.10	32.12	0.042
	22:22	32	26.55	26	27.11	27.10	32.12	0.042
	22:52	32	26.55	26	27.11	27.10	32.12	0.042
11-Mar-19								
	0:12	32	24.09	24	24.18	24.17	32.19	0.098
	0:42	32	24.09	24	24.18	24.17	32.19	0.098
	1:12	32	24.09	24	24.18	24.17	32.19	0.098
	1:43	32	24.09	24	24.18	24.17	32.19	0.098
	2:14	32	24.09	24	24.18	24.17	32.19	0.098
	2:43	32	24.09	24	24.18	24.17	32.19	0.098
	3:14	32	24.09	24	24.18	24.17	32.19	0.098
	3:44	32	24.09	24	24.18	24.17	32.19	0.098
	4:14	32	23.59	23	24.18	24.17	32.19	0.104
	4:45	32	23.59	23	24.18	24.17	32.19	0.104
	5:15	32	23.59	23	24.18	24.17	32.19	0.104
	5:45	32	23.59	23	24.18	24.17	32.19	0.104
	6:17	32	27.01	23	31.02	31.02	32.02	0.008
	6:47	32	27.01	23	31.02	31.02	32.02	0.008
	7:18	32	27.01	23	31.02	31.02	32.02	0.008

Table 4 (continued)

Date	Time, *t* min (every 30 min)	Temp.@ pt. 1 (t_1, °C)	Temp. @ pt. 2 (t_2, °C)	Temp. @ pt. 3 reading in the Arduino device (t_3, °C)	Temp. @ pt. 4 (t_4, °C)	Temp. @ pt. 5 (t_5, °C)	Room temp., t_r, °C	Thermal conductivity, k (W/m K)
	7:48	32	27.01	23	31.02	31.02	32.02	0.008
	8:19	32	27.51	24	31.02	31.02	32.02	0.007
	8:49	32	27.51	24	31.02	31.02	32.02	0.007
	9:20	32	28.01	25	31.02	31.02	32.02	0.006
	9:50	32	28.51	26	31.02	31.02	32.02	0.005
	10:32	32	29.01	27	31.02	31.02	32.02	0.005
	10:49	32	29.51	28	31.02	31.02	32.02	0.004
	11:19	32	30.01	29	31.02	31.02	32.02	0.003
	11:50	32	30.01	29	31.02	31.02	32.02	0.003
	12:20	32	30.01	29	31.02	31.02	32.02	0.003
	12:51	32	31.01	31	31.02	31.02	32.02	0.002
	13:21	32	32.01	33	31.02	31.02	32.02	0.000
	13:51	32	32.51	34	31.02	31.02	32.02	-0.001
	14:21	32	32.01	33	31.02	31.02	32.02	0.000
	14:52	32	32.01	33	31.02	31.02	32.02	0.000
	15:22	32	32.01	33	31.02	31.02	32.02	0.000
	15:52	32	31.51	32	31.02	31.02	32.02	0.001
	16:23	32	31.51	32	31.02	31.02	32.02	0.001
	16:53	32	31.51	32	31.02	31.02	32.02	0.001
	17:23	32	31.01	31	31.02	31.02	32.02	0.002
	17:54	32	31.01	31	31.02	31.02	32.02	0.002
	18:24	32	28.05	29	27.11	27.10	32.12	0.031
	18:55	32	28.05	29	27.11	27.10	32.12	0.031
	19:25	32	27.55	28	27.11	27.10	32.12	0.034
	19:55	32	27.55	28	27.11	27.10	32.12	0.034
	20:25	32	27.05	27	27.11	27.10	32.12	0.038
	20:55	32	27.05	27	27.11	27.10	32.12	0.038
	21:27	32	27.05	27	27.11	27.10	32.12	0.038
	21:57	32	26.55	26	27.11	27.10	32.12	0.042
	22:29	32	26.55	26	27.11	27.10	32.12	0.042
	22:59	32	26.55	26	27.11	27.10	32.12	0.042
	23:29	32	26.55	26	27.11	27.10	32.12	0.042
	23:59	32	26.55	26	27.11	27.10	32.12	0.042

3 Result and discussion

3.1 Experimental result of fire resistance

Tables show the result of fire resistance of different bamboo species treated with mango polyphenol extract and untreated. There are three (3) samples to determine the kind of bamboos that has higher fire resistance including the weight of bamboo before burning and ash weight after it burned. Table 1 shows that *Bambusa vulgaris* (Patong) treated with polyphenol has 15 min and 32 s where the weight of bamboo before it burned was 1880 g and weight of ash was 1010 g. However, compared with the untreated, it has rapidly burned by 25%. The treated *Dendrocalamus merrillianus* (Bayog) burned 14 min and 32 s and untreated burned of 12 min and 12 s as well, 16% faster with treated with the same weight of 1900 g and ash weight of 1100 g. The treated *Schizostachyum lumampao* (Buho) burned 11 min and 11 s compared with untreated which burned 8 min and 55 s, almost 20% faster with treated. The weight of treated and untreated bamboo was 1990 g with different weights of ash of 1210 g for treated and 1205 g for untreated. But untreated *Bumbusae* (Kawayan) was burned in 8 min and 6 s, 4% faster burning than treated which burned of 8 min and 23 s with the same weight of 1185 g and ash of 870 g.

Table 5 Average mean of thermal conductivity of bamboo plyboard at environmental temperature (t_1) of 32 °C (305.15 K)

Time, *t* (every 4 h)	1st day (March 9, 2019)	2nd day (March 10, 2019)	3rd day (March 11, 2019)	Average mean (k, W/m^2 K)
8:00 AM–12:00 AM	0.010	0.010	0.004	0.008
12:00 PM–4:00 PM	0.000	0.000	0.000	0.000
4:00 PM–8:00 PM	0.022	0.024	0.022	0.023
8:00 PM–12:00 PM	0.039	0.040	0.041	0.040
12:00 AM–4:00 AM	-	0.094	0.098	0.077
4:00 AM–8:00 AM	-	0.046	0.040	0.043
Average mean (k, W/m^2 K)	0.018	0.036	0.034	0.032

Table 2 shows that *Bambusa Vulgaris* (Patong) treated with polyphenol burned about 12 min and 12 s, and the same weight of 1600 g and burned ash was 1010 g for treated and 1020 g for untreated. The untreated has burned 18% faster than the treated with polyphenol. But, treated *Dendrocalamus merrillianus* (Bayog) burned in 11 min and 32 s, and 9 min and 17 s for untreated, which burned 20% faster. It has the same weight of untreated and treated of 1500 g as well as the weight of ash of 1000 g. The treated *Schizostachyum lumampao* (Buho) burned in 10 min and 11 s compared with untreated which burned in 8 min and 55 s, approximately 12% faster with treated. The weight of treated and untreated was 1500 g with different weights of ash of 1010 g for treated and 1005 g for untreated. However, the untreated *Bumbusae* (Kawayan) burned in 7 min and 16 s, which is 3% faster than treated which burned in 7 min and 27 s with the same weight of 1500 g and ash of 1010 g for treated and 1005 g for untreated.

The *Bambusa vulgaris* (Patong) treated with polyphenol (Table 3) burned in 12 min and 12 s and untreated in 10 min and 2 s with the same weight of 1600 g and burned ash was 980 g for treated and 970 g for untreated. It burned 18% faster than that treated with polyphenol. Although, treated *Dendrocalamus merrillianus* (Bayog) burned in 11 min and 32 s and untreated burned in 9 min and 17 s which was 20% faster. The untreated and treated has the same weight of about 1500 g and weight of ash was 860 g for treated and 840 g for untreated. The treated *Schizostachyum lumampao* (Buho) burned in 10 min and 11 s, while untreated burned in 8 min and 55 s, 12% faster with treated. The weight of treated and untreated was 1500 g, but the weight of ash for treated and untreated differs. On the other hand, the untreated *Bumbusae* (Kawayan) burned in 7 min and 16 s which was 3% faster than treated which burned in 7 min and 27 s with the same weight of 1500 g and weight of ash of about 1010 g for treated and 1005 g for untreated.

Tables 1, 2, and 3 show the result of the fire resistance of different bamboo species treated with polyphenol and untreated. The higher fire resistance determined which bamboo is going to be used for the manufacture of sawdust bamboo ply as a thermal insulator for passive roof cooling. *Bambusa vulgaris* (Patong) treated with polyphenol is the bamboo that takes so much time to burn.

3.2 Thermal conductivity of bamboo plyboard

Table 4 shows the result of the temperature at different points of the roof module within 3 days for every 30 min. Almost the result has low thermal conductivity indicating good insulating material. The temperature at pts. 1 and 2 (t_1 and t_2) is the inner and outer surface temperature of sawdust bamboo ply, temperature at pt. 3 (t_3) is the temperature reading in the Arduino device, and temperature at pts. 4 and 5 (t_4 and t_5) is the inner and outer surface of the roof. The input is the temperature reading from the

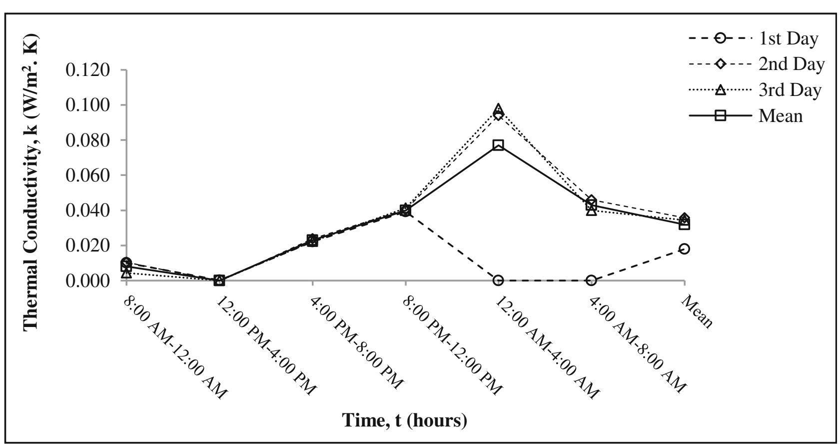

Fig. 6 Mean of thermal conductivity every 4 h on March 9 to 11, 2019

Arduino device, low and high temperature from PAGASA, and assumed room temperature of 32 °C (305.15 K). Through the empirical formula of steady-state heat transfer, the thermal conductivity is calculated.

Table 5 and Fig. 6 show the average mean of thermal conductivity of sawdust bamboo ply in every 4 h. In the 1st and 2nd day from 8:00 to 12:00 am, the mean thermal conductivity was the same of 0.010, while in the 3rd day, the mean has decreased to 0.004. In 12:00–4:00 pm, there was the same thermal conductivity in 3 trials. Then, from 4:00 to 8:00 pm, the thermal conductivity was the same for the 1st and 3rd day of 0.022 but in the 2nd day increase to 0.024. The thermal conductivity increases in

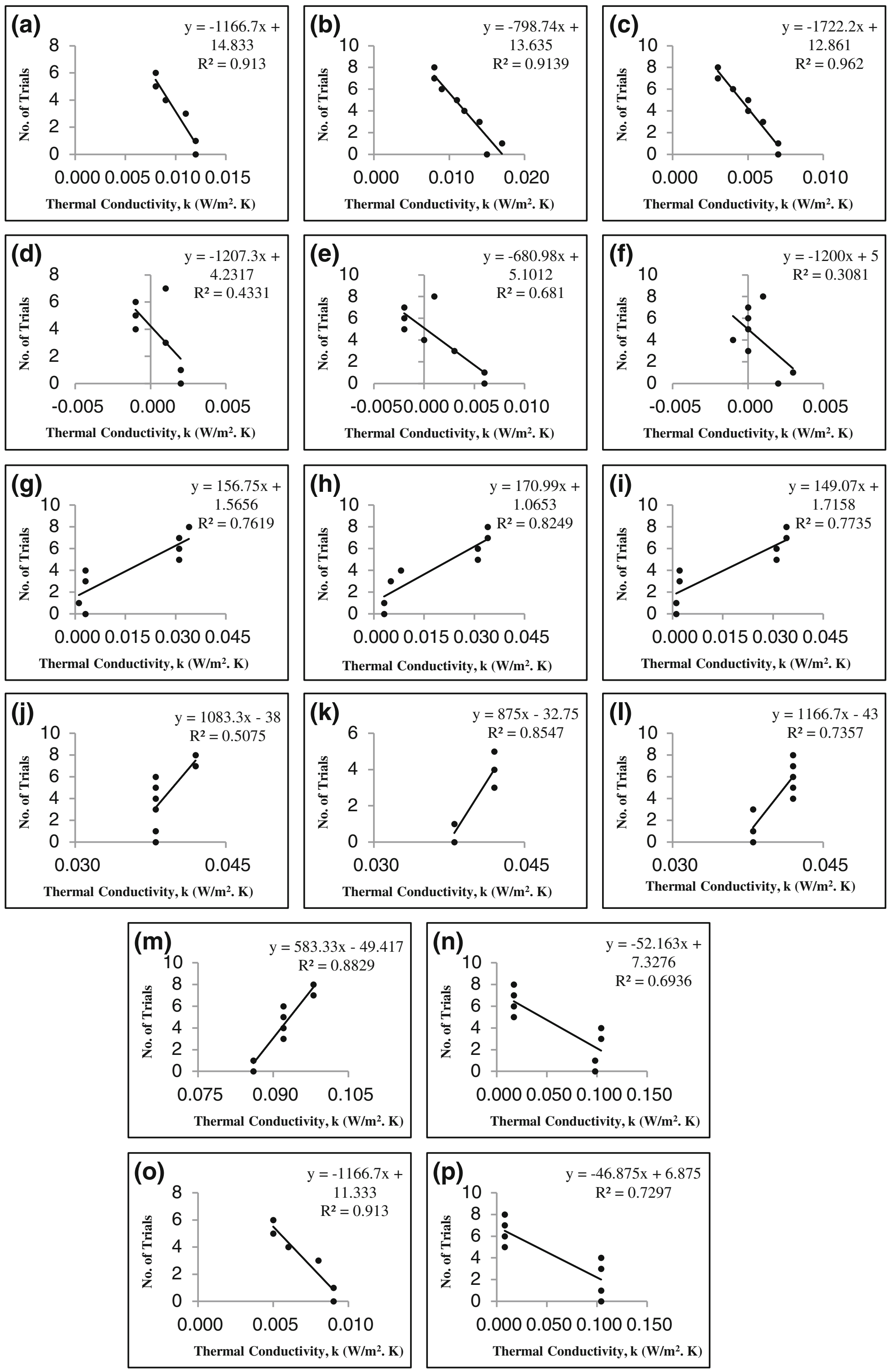

Fig. 7 Correlation ratio of thermal conductivity on March 9–10, 2019. **a**–**c** 8–12 am. **d**–**f** 12–4 pm. **g**–**i** 4–8 pm. **j**–**l** 8-12 pm. **m**, **n** 12–4 am. **o**, **p** 4–8 am

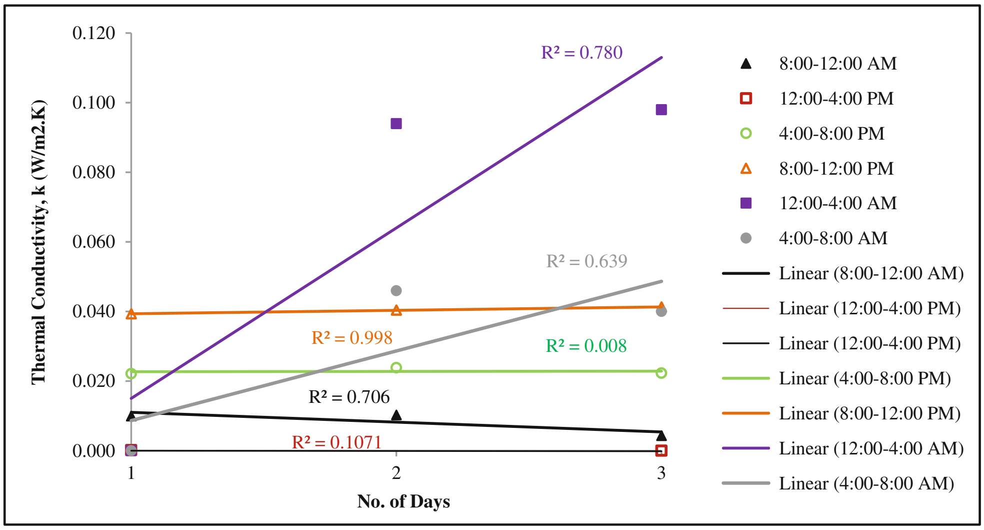

Fig. 8 Correlation ratio of thermal conductivity every 4 h

every trial from 8:00 to 12:00 pm. In 12:00–4:00 am, the thermal conductivity increases from 0.094 to 0.098, while in 4:00–8:00 am, the thermal conductivity decreases from 0.046 to 0.040.

Figure 7 shows the correlation ratio of thermal conductivity in 4 h for 3 consecutive days. Figure 7a–c show that the correlation ratio of thermal conductivity was the same on the 1st and 2nd day and slightly increase on the 3rd day; this implies that 8 to 12 am reached very high correlation. While, Fig. 7d–f show low correlation on the 1st day and 3rd day and moderate correlation on the 2nd day. Figure 7g–i show high correlation in 3 trials and Fig. 7j–l show high and moderate correlation of thermal conductivity. Figure 7m and n and Fig. 7o and p achieved of high correlation. Therefore, the thermal conductivity in every 4 h in 3 trials reached high correlation.

Figure 8 shows the average correlation ratio of thermal conductivity in 3 days for every 4 h. The correlation ratio between 8:00 and 12:00 pm has a very high correlation followed by a high correlation between 12:00–4:00 am and 8:00–12:00 am. The moderate correlation ratio is between 4:00 and 8:00 am, but the low correlation ratio is between 12:00–4:00 pm and 4:00–8:00 pm.

Figures 9, 10, and 11 show the temperature at different points of the roof module at an environmental temperature of 32 °C (305.15 K) on March 9 to 11, 2019. The temperature at point 1 was assumed as the room temperature and, at the same time, the outer surface of sawdust bamboo ply. The average inner surfaces of bamboo ply temperature in Fig. 9 were 29.08 °C (t_2), and the temperature reading from Arduino (t_3) was 29.14 °C while the inner and outer surfaces of roof (t_4 and t_5) were 29.20 °C. The low and high temperatures of bamboo ply decrease to 26.55 °C at 23:06 and increase to 32.51 °C between 14:00 and 15:00. In Fig. 10, the low and high temperatures of bamboo ply decrease to 23.59 °C between 5:10 and 5:40 am and increase to 32.52 °C between 14:16 and 15:17. The average inner and outer surfaces of the roof were 29.13 °C while the inner surfaces of bamboo ply were 29.13 °C and the temperature reading from Arduino (t_3) was 29.21 °C.

Figure 12 shows the matrix plot of the correlation ratio between the temperature of sawdust bamboo ply and temperature

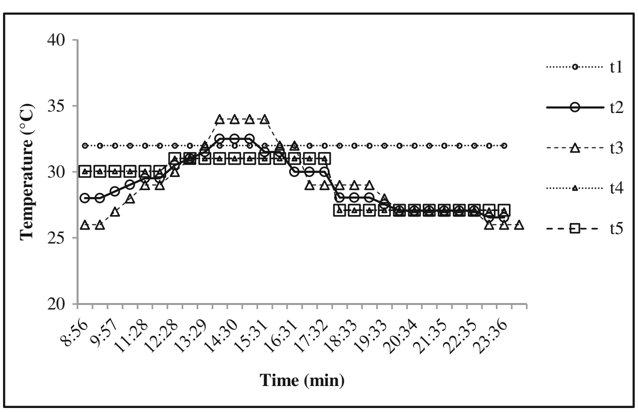

Fig. 9 Temperature at different points of the roof module at an environmental temperature of 32 °C (305.15 K) on March 9, 2019

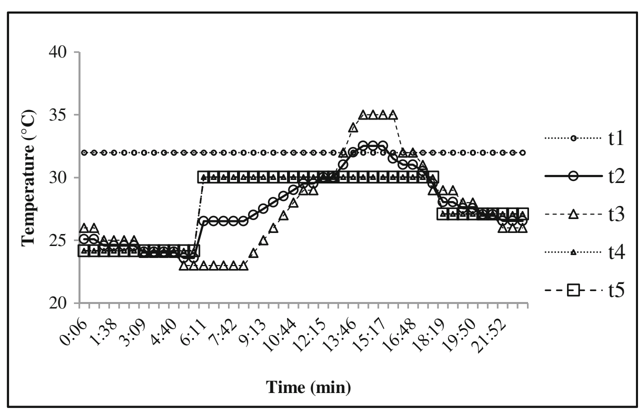

Fig. 10 Temperature at different points of the roof module at an environmental temperature of 32 °C (305.15 K) on March 10, 2019

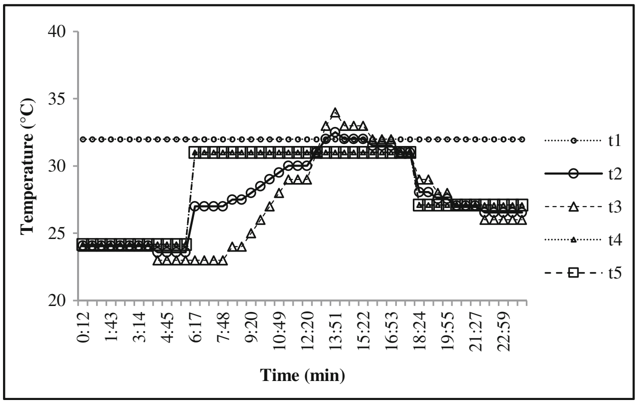

Fig. 11 Temperature at different points of the roof module at an environmental temperature of 32 °C (305.15 K) on March 11, 2019

reading from Arduino versus thermal conductivity. It shows a very high correlation ratio between temperature reading from Arduino t_3 and temperature of sawdust bamboo ply t_2 and negative high correlation between thermal conductivity (k) in W/m K and surface temperature of bamboo ply t_2 and moderate correlation with a temperature reading from Arduino t_3. The P value 0.000 ($P < 0.05$) rejects the null hypothesis; there is a significant difference between thermal conductivity and temperature of sawdust bamboo ply and temperature from Arduino device. Thus, thermal conductivity depends on the temperature gradient of the surface materials and ambient temperature.

4 Conclusion

The experiment on different fabricated samples of the nanostructured green materials [1–6] is a procedure to determine the fire-resistant quality of different bamboo species. The samples were treated with mango polyphenol extract which contains phenolic compounds such as tannin, pectin, and sodium chloride contents that affects the molecular bonds of bamboo fibers and makes molecular interlinked more stable and fire-resistant [15–23]. Comparing the treated and untreated samples of different bamboo species, the effect of treating samples was the increase in fire-resistant property by 16 to 25% based on the results of the test trials; *Bambusa vulgaris* (Patong) treated with polyphenol exhibits the highest fire resistance, about 25% higher than the untreated sample. It burned in 15 min and 32 s where the weight of bamboo prior to being burned was 1880 g and weight of ash was 1010 g for an ash content of 53.7%. In the second and third trials, it burned for about 12 min and 12 s but the weight of bamboo prior to being burned and weight of burned ash were quite different. It burned 18% faster over the untreated sample. Hence, the treated sample of *Bambusa vulgaris* (Patong) was used for the manufacture of bamboo plyboard as thermal insulation for passive roof cooling.

The study concludes that *Bambusa vulgaris* (Patong) treated with 10% mango polyphenol extract has high fire resistance; thus, it was selected for the manufacture of bamboo plyboard. The treated *Bambusa vulgaris* (Patong) thermal conductivity was

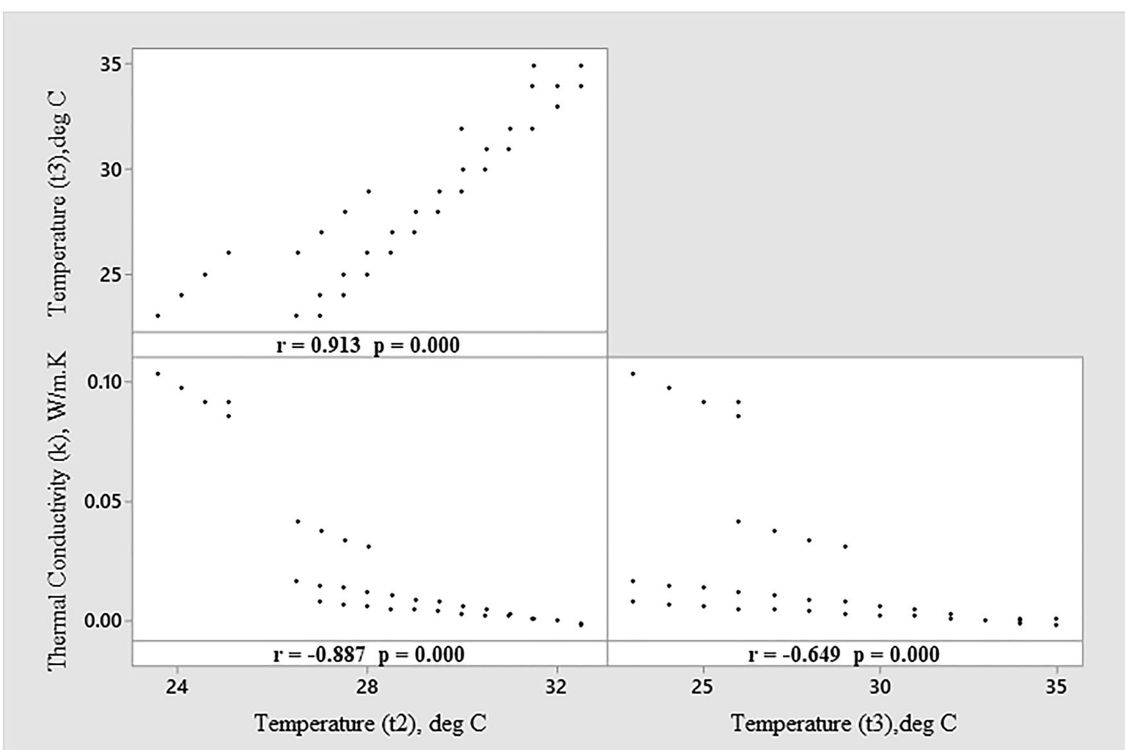

Fig. 12 Correlation ratio of matrix plot of temperature and thermal conductivity of bamboo plyboard and temperature reading from Arduino

determined employing the empirical formulas of heat transfer previously derived for roof modules. The thermal conductivity *k* ranges from 0.000 to 0.098 W/m K and the average mean is 0.032 W/m K. Based on the readings from Arduino, most thermal conductivity exhibits good correlation. The surface temperature of bamboo ply and temperature reading from Arduino were of high correlation ratio and moderate correlation between temperature readings from Arduino. The *P* value was 0.000 ($P < 0.05$), and it rejects the null hypothesis; therefore, there is a significant difference between thermal conductivity and temperature of bamboo ply and temperature from Arduino device. The average mean has shown low thermal conductivity; that is, it implies that sawdust bamboo ply made of *Bambusa vulgaris* (Patong) treated with mango polyphenol extract has good insulating value.

Thus, thermal conductivity is inversely proportional to the temperature gradient on the surface of the material and ambient temperature. The surface temperature of bamboo plyboard was obtained from the data provided by Arduino. The average inner surface temperature of bamboo ply was 29.18 °C from the empirical formula, decreased almost 9% based on an assumed room temperature of 32 °C, whereas the temperature reading from Arduino is 29.20 °C inside the roof module. The average temperature for the inner and outer surface of the roof is 29.24 °C.

Acknowledgments The authors would like to thank the Philippine Atmospheric, Geophysical and Astronomical Services Administration (PAGASA) and Weather Philippines for providing the historical climatic data. Furthermore, the authors also acknowledge the Department of Science and Technology – Engineering Research and Development Technology (DOST-ERDT), Philippines, for graduate scholarship funding.

Compliance with ethical standards

Conflict of interest The authors declare that they have no conflict of interest.

References

1. Zinatloo-Ajabshir S, Baladi M, Amiri O, Salavati-Niasari M (2020) Sonochemical synthesis and characterization of silver tungstate nanostructures as visible-light-driven photocatalyst for wastewater treatment. Sep Purif Technol 117062
2. Zinatloo-Ajabshir S, Salehi Z, Salavati-Niasari M (2018) Green synthesis and characterization of Dy2Ce2O7 nanostructures using Ananas comosus with high visible-light photocatalytic activity of organic contaminants. J Alloys Compd 763:314–321
3. Zinatloo-Ajabshir S, Morassaei MS, Amiri O, Salavati-Niasari M, Foong LK (2020) Nd2Sn2O7 nanostructures: green synthesis and characterization using date palm extract, a potential electrochemical hydrogen storage material. Ceram Int
4. Zinatloo-Ajabshir S, Morassaei MS, Salavati-Niasari M (2018) Nd2Sn2O7 nanostructures as highly efficient visible light photocatalyst: green synthesis using pomegranate juice and characterization. J Clean Prod 198:11–18
5. Zinatloo-Ajabshir S, Morassaei MS, Amiri O, Salavati-Niasari M (2020) Green synthesis of dysprosium stannate nanoparticles using Ficus carica extract as photocatalyst for the degradation of organic pollutants under visible irradiation Ceramics International 46(5) 6095-6107
6. Zinatloo-Ajabshir S, Ghasemian N, Salavati-Niasari M (2020) Green synthesis of Ln2Zr2O7 (Ln = Nd, Pr) ceramic nanostructures using extract of green tea via a facile route and their efficient application on propane-selective catalytic reduction of NOx process. Ceram Int 46(1):66–73
7. Martin M, Berdahl P (1984) Characteristics of infrared sky radiation in the United States. Sol Energy 33(3-4):321–336
8. Parker DS (2005) Theoretical evaluation of the night cool nocturnal radiation cooling concept. Submitted to: US Department of Energy. FSEC-CR-1502-05
9. Çengel YA, Turner RH, Cimbala JM, Kanoglu M (2001) Fundamentals of thermal-fluid sciences, vol 703. McGraw-Hill, New York
10. Cengel YA (2006) Heat and mass transfer: a practical approach. 3rd Ed. (SI units) McGraw-Hills Companies, Inc.
11. ASHRAE 2009: Psychrometrics. Handbook and Fundamentals
12. Flander KD, Rovers R (2009) One laminated bamboo-frame house per hectare per year. Constr Build Mater 23(1):210–218. https://doi.org/10.1016/j.conbuildmat.2008.01.004
13. Huang P, Chang WS, Shea A, Ansell MP, Lawrence M (2014) Non-homogeneous thermal properties of bamboo, In Materials and joints in timber structures (pp. 657-664). Springer Dordrecht.
14. Mena J, Vera S, Correal JF, Lopez M (2012) Assessment of fire reaction and fire resistance of Guadua angustifolia Kunth bamboo. Constr Build Mater 27(1):60–65
15. Soto ML, Moure A, Domínguez H, Parajó JC (2011) Recovery, concentration and purification of phenolic compounds by adsorption: a review. J Food Eng 105(1):1–27
16. Casas MP, Soto ML, Díaz RB, Balboa EM, Moure A, Conde E, Parajó JC (2016) 7 Purification of polyphenolic. Advances in technologies for producing food-relevant polyphenols 163
17. Gouw VP (2016) Investigation of bioactive compounds in different types of fruit pomace and their applications as bulk materials for creating biocomposite.
18. Basak S, Ali SW (2018) Fire resistant behaviour of cellulosic textile functionalized with wastage plant bio-molecules: a comparative scientific report. Int J Biol Macromol 114:169–180
19. Kandola BK, Krishnan L, Deli D, Ebdon JR (2015) Blends of unsaturated polyester and phenolic resins for application as fire-resistant matrices in fibre-reinforced composites. Part 2: Effects of resin structure, compatibility and composition on fire performance. Polym Degrad Stab 113:154–167
20. Partansky AM (1966) U.S. Patent No. 3,252,850. Washington, DC: U.S. Patent and Trademark Office.
21. Xia Z, Kiratitanavit W, Facendola P, Thota S, Yu S, Kumar J, Nagarajan R (2018) Fire resistant polyphenols based on chemical modification of bio-derived tannic acid. Polym Degrad Stab 153: 227–243
22. Leopold B H (1954) U.S. Patent No. 2,680,102. Washington, DC: U.S. Patent and Trademark Office.
23. Paire C (1993) U.S. Patent No. 5,236,769. Washington, DC: U.S. Patent and Trademark Office